On the pool boiling heat transfer enhancement of distilled water using Cu-nanoparticles textured with carbon nanofibers

Mohamed R. O. Ali (mohamedroali@mu.edu.eg)
Minia University
Nasser A. M. Barakat
Minia Univeristy
Ramadan Bassiouny
Minia University
Ibrahim M. M. El Moghazy
Minia University
Mahmoud M. S. Ragab
Minia University

Research Article

Keywords: Pool boiling enhancement; Heat Transfer; Electrospinning; Nanofibers; Cu-incorporated carbon nanofibers

Posted Date: May 20th, 2020

DOI: https://doi.org/10.21203/rs.3.rs-29438/v1

Abstract

Enhancement of subcooled and saturation pool boiling is of interest for many applications. The present study proposes coating heated surface using nanotextured of Cu nanoparticles with carbon nanofibers. This texture formation on copper substrate surface passes through different chemical stages under specific conditions. Using electrospinning, coating was carried out at different times (5, 15, and 30 min). After vacuum drying at 60 ^{o}C for 24 h, the copper substrates attaching the electrospun mat were calcined at 850 ^{o}C under vacuum. and accordingly, different contact angles were measured as 80^{o}, 115^{o}, and 102^{o}. The coated surfaces are coded by S1, S2 and S3 for the electrospun coated surfaces of (5, 15, and 30), respectively.

All nanostructured coated surfaces showed a good heat transfer enhancement compared to uncoated copper surface for both HTC and CHF. The results showed an enhancement of HTC by 57.83%, 40.3% for S2 and S3 respectively and an enhancement of CHF by 13.67%, 17.11% and 48.14% for S1, S2 and S3 respectively.

1. Introduction

Electronic devices and microelectronics are generating high heat flux, so cooling plays a major role since the operating temperature affects the performance of these devices. Several cooling techniques of microelectronics have been applied such as single-phase liquid cooling, spray cooling, jet impingement cooling, heat pipes, liquid metal cooling, indirect cooling with phase change materials, flow boiling and pool boiling[1]{Anderson, 1989 #5}{Anderson, 1989 #5}{Anderson, 1989 #5}. Pool boiling is an efficient mechanism for heat transfer due to the associated phase change process, with the demand for meeting high heat flux removal in excess of 10 MW/m^{2}. Mouromtseff and Kozanowski[2] early noted the actual application of boiling in electronics applications.

Boiling heat transfer plays an important role in several thermal devices such as boilers, heat exchangers, and condensers etc. One of the most important parameters of boiling heat transfer is the critical heat flux (CHF) that is very important factor for thermal device safety. Critical heat flux means that when the heat supplied for boiling reaches a certain point , the temperature of the heated surface suddenly increases and hence a deterioration in heat transfer occurs[3]. Therefore, CHF should be controlled since it has a significant impact on energy conversion and utilization in thermal systems. Additionally, the enhancement and augmentation of pool boiling heat transfer can lead to the reduction of the size of cooling surfaces and compactness (material saving). In general, heat transfer enhancement techniques can be classified as active, passive, and compound Techniques[4]. In the active technique, an external power is needed to improve the overall heat transfer of the system, while in the passive technique, no external power is required. On the other hand, the compound technique includes both active and passive

techniques at the same time. Passive techniques have higher reliability, as compared to active techniques, due to the absence of moving components and auxiliary power[5].

During the past few decades, researchers have been focusing their studies in the pool boiling heat transfer enhancement through treated surfaces methods by coating with micro to nanoscale material. This is an important passive technique. Different coating techniques for boiling heat transfer enhancement are found in the literature such as, sintering[6], spraying[7], plasma coating[8] and electrochemical deposition[9]. They used different materials such as metals, polymers, ceramics, and composites for complex geometries with different shapes such as 3D porous structures, pyramids, bumps and pillars in micro-nanoscales. The boiling heat transfer performance is affected by the properties of the boiling surface such as material, geometry, nucleation sites, porosity, roughness and orientation.

Three major parameters affecting the enhancement of boiling process are the existence of random micro- or nano-size cavities, surface irregularities for nucleation initiation, porous surface structure that allows fluid inflow to keep nucleation sites active, and surface protrusions that create more active boiling area.

While many of the previous studies on the heated surface structure focused on improving the heat transfer coefficient of pool boiling in micro-sized dimensions, the emergence of nanotechnology science attracts many researchers. The expected advantages of nanoscale modifications include finer control over porosity and surface roughness, thinner coating layers to reduce the thermal resistance and thermal stress and ultimately results in higher durability. Most of the studies have focused on CHF enhancement by using nanostructured surfaces[10].

Recently, there has been an increased interest in evaluating pool boiling performance using nanowire, nanofiber, and nanotube surfaces[11], which revealed promising results of boiling heat transfer coefficient (BHTC) and critical heat Flux (CHF) enhancement.

Table 2.8 Various studies on pool boiling heat transfer enhancement using surfactants and polymer additives (Wasekar and Manglik 2018)

Author(s)	Heater geometry and heat flux level (kW/m^2)	Additives	Effect on heat transfer
		Surfactant solutions:	
Morgan et al. (1949)	Cylinder 0–500	Drene (triethanolamine alkyl sulphate), and sodium lauryl sulphonate	Enhances heat transfer with a maximum of around 100%
Jontz and Myers (1960)	Plate 20–25	Tergitol (sodium tetradecyl sulphate), and aerosol-22 (*n*-octadecyl tetrasodium 1,2 dicarboxyethyl sulphosuccinamate)	Heat transfer coefficient enhancement to the extent of 50%
Podsushnyy et al. (1980)	Cylinder 0–80	PVS-6 polyvinyl alcohol, NP-3 sulphonol, and SV 1017 wetting agent	Enhancement has an optimum value for concentration corresponding to c.m.c. In the higher heat flux range, the enhancement is higher for larger size heater
Filippov and Saltanov (1982)	Cylinder 0–100	Octadecylamine	Heat transfer coefficient improved by 100%
Yang and Maa (1983)	Plate 0–600	SLS (sodium lauryl sulphate), and SLBS (sodium lauryl benzene sulphonate)	Maximum enhancement of 100–200% in the nucleate boiling regime, and a 50–100% increase in critical heat flux Also, the enhancement depends on particular surfactant in solution
Saltanov et al. (1986)	Cylinder 40–120	Octadecylamine	Maximum enhancement to the extent of 100% for an optimum level of additive concentration
Tzan and Yang (1990)	Cylinder 0–400	SLS (sodium lauryl sulphate)	Enhanced with a maximum increase of around 200% with an optimum value of surfactant concentration at high heat fluxes (>300 kW/m^2)
Liu et al. (1990)	Plate 0–400	BA-1, BA-2, BA-3, BA-4, DPE-1, DPE-3. Gelatine, oleic acid, trimethyl octadecyl ammonium chloride, trialkyl methyl ammonium chloride, and polyvinyl alcohol	Maximum enhance item in die range of 200–700% observed with BA-1, BA-2 and BA-3, while no effect with other additives

(continued)

Literature showed many coating morphologies of nanostructures that are deposited and coated on surfaces using different techniques and applied to pool boiling heat transfer enhancement such as nonporous[12], nanoparticle thin film[13], nanowires[14], nano rods[15], nanofibers[16], nanofins[17], flower-like nanostructures[18] and, nano tubes coated surfaces[19].

Sudev Das et al[20] discussed the effect of nanoparticle thin film coating of silicon oxide on copper surfaces using electron beam physical vapor deposition technique. They experimentally concluded that a 58% enhancement in the boiling heat transfer coefficient and a reduction of about 36% in the superheat inception for coated surface was noticed compared to the plain one.

Ali et al.[21] discussed the enhancement of pool boiling heat transfer of distilled water on TiO_2 nanoparticles coated copper surface. They used a nanofluid boiling coating technique. An enhancement of HTC by 38% was recorded. Dareh et al.[22]deposited Al_2O_3 nanoparticles on polished surface and Cu machined surface using nanofluid boiling and tested the coated surfaces in pool boiling of water. An enhancement up to 37% in HTC and 7% in CHF was obtained by coated surface compared to the

uncoated one. Jaikumar[23] experimentally studied the pool boiling on Cu surface covered with GO and Cu particles coating using screen printing and electrodeposition technique .An enhancement up to 1.8 times in CHF, and 2.4 times in HTC for coated surfaces was noticed compared to plain one. A. Jaikumar [24] studied pool boiling of water on cupper surfaces coated with Cu and graphene nanoparticles. The results showed a HTC enhancement of 82% compared to smooth copper surface. Seo et al.[25] experimentally studied pool boiling of deionized water stainless steel substrate coated with SWCNT. The results showed an increase of CHF by 55% on coated surface compared to a polished surface. Pialago et al.[26] studied pool boiling of R134a on Cu surface covered with Cu–CNT–Sic, Cu–CNT–AlN using mechanical alloying and cold gas dynamic spraying. It was concluded that a 148% enhancement by The Cu–CNT coating compared to bare copper surface. Ray et al.[27] investigated the effect of TiO_2 Nano wire arrays coated copper surface on pool boiling of R-134a. The coating was manufactured using E-beam evaporation technique. It was concluded an enhancement in both HTC and CHF. Jo *et al*.[28] experimentally studied the effect of Silver Nano wires sprayed on copper surface, using supersonic spraying technique, on the enhancement of pool boiling of water. The results showed an enhancement of CHF and HTC. They studied the bubble dynamics using a high-speed camera. Lee *et al*.[29] investigated the pool boiling heat transfer enhancement of water on stainless steel surface covered with polyethylenimine multi-walled carbon nanotube. The coating was fabricated using layer by-layer assembly technique. A 147% enhancement of CHF compared to the bare surface was obtained.

Recently, in pool boiling there are many methods for coating nanofibers on surfaces. Metal-plated electro spun nanofiber mats used to enhance heat removal in pool boiling while rough, metal-plated nanofibers act as nucleation sites, simultaneously increase the number of bubbles and their growth rate[30]. Another method known as supersonic solution blowing[31] was used to developing nanofibers even smaller than the electro spun ones. These nanofibers, being metal-plated, revealed a much better robustness than their electro spun counterparts and could withstand delamination from the heater surface even after multi-hour vigorous pool boiling[32]. They also removed higher heat fluxes at lower surface superheats, and were able to delay the onset of CHF[32].

The objective of this work is to study pool boiling heat transfer performance at atmospheric pressure using nanostructures coating on the heated surface. Copper nanoparticles incorporated carbon nanofibers are tested through surface coating. The effects of carbon nanofibers properties are further investigated with respect to wettability, coating thickness as a function of electro spinning time at specified voltage, and coating morphology and topography.

2. Experimental Set-up

The experimental facility shown in Fig.1, consists of a thick, Pyrex glass, boiling chamber of nearly one-liter capacity. It is 140 mm diameter and 220 mm height. Inside this chamber there is a guard heater of 500 W. A type K thermocouple is attached to a PID controller to control the saturation temperature during the experiment. There is a glass condenser which is open to the atmosphere to ensure atmospheric pressure inside the boiling chamber and to condensate water vapor and maintain a constant level of

water for all experiments. A thick cover of Plexiglass of the boiling chamber with holes for the condenser, thermocouple and guard heater. Beneath the boiling chamber there is a thick insulated Teflon plate of 210 mm in diameter and 20 mm thickness to carry the tested system. This plate has a 60 mm diameter hole at the center to facilitate the removal and insertion of the test samples. A copper heating element with base diameter of 30 mm and height of 105 mm tapered to a diameter of 15 mm and a height of 35 mm to approximate a dimensional axial heat transfer. A copper substrate of 15mm diameter and 20 mm height was fitted on the surface. A very thin layer of high thermal conductive grease was placed between the heater and the tested substrate to minimize thermal contact resistance. Three cartridge heaters, of 500 W each are fitted inside the copper rod. Type-K thermocouples are properly placed as shown in Fig. 1(b). A Teflon ring was fitted around the substrate for sealing. High-temperature thermal insulation material was used to cover the whole heating system to reduce the heat loss to the surrounding ambient. All thermocouples were attached to data acquisition system (mini logger GL 240) to instantaneously help recording required temperature values.

3. Samples Preparation

Electrospinning technique involves the use of a high voltage to charge the surface of a polymer solution droplet and thus to induce the ejection of a liquid jet through a spinneret. Due to bending instability, the jet is subsequently stretched by many times to form continuous ultra-thin fibers was used[33].

The electro spun sol-gel is formed by mixing of CuAc solution (20 wt% in water) with a pre-prepared PVA aqueous solution (10 wt %). The final mixture was adjusted to have 20 wt% of the metallic precursor with respect to the solid polymer. The mixture was vigorously stirred at 50 ^{o}C for 5 h. The final prepared solution was placed in a plastic capillary. The formed polymeric nanofibers were collected on the surface of the copper specimen. The electrospinning process was carried out at 20 kV with a tip-to-collector distance of 25 cm. Three polished surfaces were coated with different electrospinning time (5, 15, and 30 min). The samples are labeled as S1, S2 and S3. The specimens holding the formed nanofibers were initially dried at 60 ^{o}C for 24 h under vacuum. Then, the copper substrates were calcined at 850°C for 2 h under vacuum with a heating rate of 3 °C/min.

The surface morphology was studied by scanning electron microscope (JSM IT 200). Information about the phase and crystallinity was obtained by using x-ray diffractometer. High-resolution image and selected area electron diffraction patterns were obtained with transmission electron microscope.

4. Testing Procedure

The boiling chamber was filled by a one-liter distilled water, then the guard heater is turned on until water reaches the saturation temperature. Hence cartridge heaters are turned on at a specified voltage. To eliminate the effect of non-condensable gases, guard heater is turned on for 1 hour. Voltage is increased gradually by an increment of 7 volts, then the system is left to reach steady state in each increment. When approaching CHF, voltage was increased by a small increment. When abrupt increase in

temperatures of all system occurs, hence the CHF was reached, and the all system must be shut down. CHF was assumed to be the last quasi steady heat flux before the occurrence of the abrupt increase of temperatures. Steady state takes almost 1.5 hours at each voltage increment. Steady state was reached when all thermocouples were fluctuating (± 0.2^{o}C) in 10 mins.

Five K-type thermocouples with 1.5 mm in diameter and accuracy of 0.2 K, were imbedded along the vertical axis of the heated rod to interpolate the boiling surface temperature and linear estimate the heat flux. Linear temperature profiles over the copper rod for different heat fluxes show the heat generated from the cartridge heater was transferred to the test section through 1D conduction and there is no heat loss in thermocouple's block section.

The uncertainty of the measurement parameters are analyzed by the Kline and McClintock method[34], the Uncertainty of heat flux is ±14%. Also, Uncertainty of instruments used in this study as follows, K-Type thermocouple to measure Temperature (°C), (calibrated) range (−50 – 1000°C) is ±0.2°C , DT266 CE Digital clamp meter to measure voltage (V) is ±1% and DT266 CE Digital clamp meter to measure current (A) is ±0.1%.

5. Results And Discussion

Fig. 2 displays the SEM image of the collected nanofibers before the calcination process. As shown, smooth and beads-free nanofibers were obtained.

Fig. 3 shows SEM images of the copper specimen surfaces after the calcination process. Fig. 3A shows the SEM image of the specimen surface coated for 5 min; S1. As shown, small amount of nanofibers appeared and a microporous nanostructure. Fig 3B and 3C show the morphology of S2 and S3 samples, respectively. As it can be concluded, increasing the electrospinning time leads to an increase in the nanofibers density on the surface. Fig 4 displays the EDX analysis of the surface S3. The copper identification peaks clearly appear.

Compared to many polymers, the carbon content in the PVA is relatively high. However, it is not commercially used as a precursor of carbon nanofibers fabrication due to the problem of breaking down to volatile compounds before the graphitization process. However, presence of metal nanoparticles can distinctly overcome this dilemma[35, 36]. Fig. 5 demonstrates the XRD pattern for the obtained nanofibers after the calcination process. The obtained results confirmed formation of pure copper due to appearance the standard peaks representing (111), (200), (220), (311) and (222) crystal plans (JCDPS # 04-0836). Moreover, the appeared broad peak at 2theta value ~ 26^{o} is attributed to formation of graphite phase. The results indicated that the obtained nanofibers composed of zero valent copper (Sp.Gr Fm3m (225)). The inset demonstrates the TEM image of the obtained nanofibers. The image indicates that the obtained nanofibers compose of amorphous nanofiber matrix embedded crystalline nanoparticles. Accordingly, it can be confidently concluded that the final product is copper nanoparticles-incorporated carbon nanofibers.

In order to validate the accuracy and reliability of the experimental set up, experiments were carried out on coated and noncoated surfaces to compare pool boiling behavior. Pool boiling experiments were first conducted on the polished copper substrate. The plain copper surfaces were finally polished with a 2500 grit sandpaper successively. In this study, nanostructured surfaces is to be compared with a smooth surface.

The degree of superheat , ΔT, and heat flux (q) were compared with the commonly popular used Rohsenow correlation [37] which considers the influence of the liquid solid combination on boiling heat transfer.

$$q = \mu_f h_{fg} \left[\frac{g(\rho_f - \rho_g)}{\sigma}\right]^{\frac{1}{2}} \left[\frac{C_{pf}\Delta T}{C_{sf} h_{fg} Pr_f^{\,n}}\right]^3 \quad (4)$$

Fig. 6 compares the present results and Rohsenow correlation in case of smooth copper surface. The results showed a good agreement between the experiments and correlation with a small deviation.

There are many proposed models to predict CHF such as Zuber [38], and Kandlikar's model [39]. Zuber's model is based on the hydrodynamic instability theory but doesn't consider the effect of surface structure and wettability. He predicted the critical heat flux for water as 110 W/cm^2 in atmosphere pressure. Equation 5 shows Zuber's model:

$$q = \frac{\pi}{24} h_{fg} \rho_f^{0.5} \left(\sigma g(\rho_f - \rho_g)\right)^{0.25} \quad (5)$$

The Prediction of this model [38] is slightly higher than the results for the polished surface measured in the present study. This is attributed to the fact that the models based on the hydrodynamic instability theory does not consider the surface wettability and heater size effect. Kandlikar's[39] model considered the hydrodynamic instability theory by including the wettability effect and surface inclination factor, as follows:

$$q = h_{fg} \rho_g^{\frac{1}{2}} \left[\frac{1 + cos\beta}{16}\right] \left[\frac{2}{\pi} + \frac{\pi}{4}(1 + cos\beta) cos\varphi\right]^{\frac{1}{2}} \left[\sigma g(\rho_f - \rho_g)\right]^{\frac{1}{4}} \quad (6)$$

In fact, Polymer nanofibers have lower thermal conductivity[40]. Through the boiling of water on polymer electro spun nanofibers coated surfaces, detachment of nanofibers occurs [16]. So, in present study, calcination process was applied on the test samples to convert electro spun polymer nanofibers to carbon nanofibers which have higher thermal conductivity and to make self-sintering to nanofibers and thus enhance the mechanical stability of the coating. The copper nanoparticles which are embedded in the carbon nanofibers are sintered with the original copper surface that enhances the mechanical stability and this prevents the detachment of nanofibers from the heating surfaces through vigorous boiling. Wettability effect on the heating surfaces in the boiling phenomenon has a great effect in the enhancement mechanism. In the present study contact angles are measured using a contact angle

goniometer. For a contact angle of the smooth surface of 70^{o}. The nanostructured surfaces in this study revealed hydrophilic structure for S1 and hydrophobic structures for S2 and S3 with a contact angles of 80.65^{o}, 115^{o}, 102^{o} for the three samples respectively. Fig. 7 shows the contact angles for the samples. Smooth surface and S1 have higher wettability but Surfaces S2 and S3 have lower wettability. The hydrophobicity of surfaces S2 and S3 is due to the combined effect of copper Nano particles and carbon nanofibers. Fig. 8 shows the effect of electro spinning time on contact angles.

Fig. 9 shows the boiling curves of heat flux (q) versus wall superheat ( ) for a smooth surface baseline compared to nanostructured surfaces. The nanostructured surfaces showed a noticeable enhancement in the heat transfer coefficient (HTC) and Critical heat flux (CHF) compared to the smooth surface. Surface S3 showed a 48.14% enhancement in the CHF which is higher compared to S1 and S2.

Fig. 10 shows the variation of heat transfer coefficient against the heat flux for nanostructured surfaces compared to the smooth surface. The nanostructured surfaces revealed a significant enhancement in the effective heat transfer coefficient at each heat flux. Surface S2 and S3 have 57.83% and 40.3% enhancement. While surface S1 has a wall superheat reduction of 4.8 ^{o}C compared to smooth surface at low heat flux. The enhancement mechanism of the nanostructured surfaces can be attributed to that the structure surfaces of the copper Nano particles incorporated carbon nanofibers having more surface area to volume and tremendous Nano-size cavities. A more active nucleation site at the nanotextured surfaces compared to the smooth surface contributed to the overall heat transfer enhancement. This enhancement can be expected because of the departure frequency of bubbles which were generated from nanostructured surfaces. This frequency is significantly higher than those from the bare surface due to the increase of contact angle and hydrophobic characteristics of the nanostructured surfaces.

Bubble release is more efficient for hydrophobic Surfaces[41-43]. Early onset of boiling is obtained for nanostructured samples compared to the smooth copper sample due to higher nucleation density. This effect is due to the hydrophobicity and high relative roughness for nanostructured surfaces.

This means that at a certain time interval more bubble will generate and depart from the nanostructured surfaces and leads to heat transfer enhancement. Although S3 has the larger time of collected fibers and expected larger roughness but the increase of coating thickness as a function of electrospinning time cause the intermediate thermal resistance to slightly increases compared to S2 and hence S2 has higher heat transfer coefficient enhancement than S3. Due to the increase of electrospinning time and the accumulation of collected nanofibers with copper Nano particles, more roughness and more increase in the surface area is expected, hence S3 recorded the highest enhancement in critical heat flux CHF enhancement of 48.14% compared to smooth surface.

Fig. 11 shows the relation between CHF and electrospinning time. As shown, CHF increases with increasing coating thickness as a function of electrospinning time. Also, SEM images revealed that the three coated surfaces have micro porous surfaces which is a good environment structure for bubble nucleation.

6. Conclusion

An experimental study was conducted to investigate the pool boiling heat transfer performance when using copper nanoparticles incorporated carbon nanofibers coated surfaces. Electrospinning time is the effective parameter in this study that shape the surface, and hence affects its wettability. Nanostructured surfaces showed a noticeable enhancement compared to smooth surface. An enhancement in heat transfer coefficient by 57.83% and a 17.15% enhancement in CHF was obtained for S2 surface. Surface S1 showed an enhancement of 13.67% in CHF. Surface S3 indicated 48.14% enhancement in CHF and an enhancement of 40.3% in the heat transfer coefficient. This means that the increase of electrospinning time leads to a slight deterioration in the heat transfer coefficient because of the increase of intermediate thermal resistance between the Nano coating and the original surface. Copper nanoparticles embedded in carbon nanofibers significantly improves the mechanical and thermal stability of the nanostructured coatings.

Abbreviations

Nomenclature

CHF	critical heat flux, W/m^2
C_{pf}	specific heat of liquid, J/kg.°C
C_{sf}	experimental constant that depends on surface –fluid combination
g	gravitational acceleration, m/s^2
HTC	heat transfer coefficient, $W/m^2.°C$
h_{fg}	enthalpy of vaporization, J/kg
n	experimental constant that depends on fluid
Pr_f	prandtl number of liquid
q	heat flux, W/m^2
ΔT	wall superheat temperature, °C

Greek symbols

ρ_f	density of liquid, kg/m^3
ρ_g	density of vapor, kg/m^3
σ	surface tension of liquid vapor interface, N/m
μ_f	viscosity of liquid, kg/m.s
β	receding contact angle, °
φ	surface inclination angle, °
Θ	static contact angle, °

Declarations

Competing interests: The authors declare no competing interests.

References

[1] T. Anderson and I. Mudawar, "Microelectronic cooling by enhanced pool boiling of a dielectric fluorocarbon liquid," *Journal of Heat Transfer,* vol. 111, pp. 752-759, 1989.

[2] I. Mouromtseff and H. Kozanowski, "Comparative analysis of water-cooled tubes as class B audio amplifiers," *Proceedings of the Institute of Radio Engineers,* vol. 23, pp. 1224-1251, 1935.

[3] S. S. Kutateladze and . " Fundamentals of Heat Transfer,," *Academic Press, New York,* 1963.

[4] A. Bejan and A. D. Kraus, *Heat transfer handbook* vol. 1: John Wiley & Sons, 2003.

[5] G. Paul, M. Chopkar, I. Manna, and P. Das, "Techniques for measuring the thermal conductivity of nanofluids: a review," *Renewable and Sustainable Energy Reviews,* vol. 14, pp. 1913-1924, 2010.

[6] S. Jun, J. Kim, S. M. You, and H. Y. Kim, "Effect of heater orientation on pool boiling heat transfer from sintered copper microporous coating in saturated water," *International Journal of Heat and Mass Transfer,* vol. 103, pp. 277-284, 2016.

[7] S. K. An, D.-Y.; Lee, J.-G.; Jo, H.S.; Kim, M.; Al-Deyab, S.S.; Choi, J.; Yoon, S.S, "Supersonically sprayed reduced graphene oxide film to enhance critical heat flux in pool boiling," *Int. J. Heat Mass Transf,* vol. 98, pp. 124–130, 2016.

[8] S. K. Das, D.S.; Bhaumik., S, "Experimental study of nucleate pool boiling heat transfer of water on silicon oxide nanoparticle coated copper heating surface," *Appl. Therm. Eng,* vol. 96, pp. 555–567, 2016.

[9] K. S. V. S. Z. Protich, A. Jaikumar, S. G. Kandlikar, and P. Wong, "Electrochemical Deposition of Copper in Graphene Quantum Dot Bath: Pool Boiling Enhancement *J. Electrochem. Soc,* vol. 163(6), pp. 166-E172, . 2016

[10] T. J. Dinh N., Theofanous T, "Hydrodynamic and physico-chemical nature of burnout in pool boiling," *Proc. 5th Int. Conf. on Multiphase Flow*,*Yokohama, Japan.,* 2004.

[11] S. A. Khan, " Study of CNF Coating for Pool-Boiling and Condensation. " *InProceedings of the International Conference on Sustainable Energy and Environmental Protection, Changsha*,*China,* vol. 23-25, pp. 27–30, June 2017.

[12] B. J. Zhang, "Enhanced heat transfer performance of alumina sponge-like nano-porous structures through surface wettability control in nucleate pool boiling," *International Journal of Heat and Mass Transfer,* vol. 55 pp. 7487–7498, 2012.

[13] S. D. e. al, "Experimental study of nucleate pool boiling heat transfer of water on silicon oxide nanoparticle coated copper heating surface," *Applied Thermal Engineering* vol. 96, pp. 555–567, 2016.

[14] B. Shi, "Pool boiling heat transfer enhancement with copper nanowire arrays "*Applied Thermal Engineering* vol. 75 pp. 115 -121, 2015.

[15] E. Demir, "Effect of silicon nanorod length on horizontal nanostructured plates in pool boiling heat transfer with water" *International Journal of Thermal Sciences* vol. 82, pp. 111-121, 2014.

[16] S. Sinha-Ray, "Pool boiling of Novec 7300 and DI water on nano-textured heater covered with supersonically-blown or electrospun polymer nanofibers," *International Journal of Heat and Mass Transfer* vol. 106, pp. 482–490, 2017.

[17] S. R. SRIRAMAN, "POOL BOILING ON NANO-FINNED SURFACES ", Office of Graduate Studies of Texas A&M University, December 2007

[18] C. D. Yunhyeok Im , Seung S. Lee & Yogendra Joshi "Flower-Like CuO Nanostructures for Enhanced Boiling "*Nanoscale and Microscale Thermophysical Engineering* vol. 16:3, pp. 145-153, 2012.

[19] J. P. McHale, "Pool Boiling Performance Comparison of Smooth and Sintered Copper Surfaces with and Without Carbon Nanotubes " *Nanoscale and Microscale Thermophysical Engineering* vol. 15, pp. 133-150, 2011.

[20] S. Das, D. Kumar, and S. Bhaumik, "Experimental study of nucleate pool boiling heat transfer of water on silicon oxide nanoparticle coated copper heating surface," *Applied Thermal Engineering,* vol. 96, pp. 555-567, 2016.

[21] H. M. Ali, M. M. Generous, F. Ahmad, and M. Irfan, "Experimental investigation of nucleate pool boiling heat transfer enhancement of TiO2-water based nanofluids," *Applied Thermal Engineering,* vol. 113, pp. 1146-1151, 2017.

[22] F. R. Dareh, M. Haghshenasfard, M. N. Esfahany, and H. S. Jazi, "Experimental investigation of time and repeated cycles in nucleate pool boiling of alumina/water nanofluid on polished and machined surfaces," *Heat and Mass Transfer,* vol. 54, pp. 1653-1668, 2018.

[23] A. Jaikumar, A. Rishi, A. Gupta, and S. G. Kandlikar, "Microscale morphology effects of copper–graphene oxide coatings on pool boiling characteristics," *Journal of Heat Transfer,* vol. 139, p. 111509, 2017.

[24] A. Jaikumar, K. S. Santhanam, S. G. Kandlikar, I. Raya, and P. Raghupathi, "Electrochemical deposition of copper on graphene with high heat transfer coefficient," *ECS Transactions,* vol. 66, pp. 55-64, 2015.

[25] G. H. Seo, H. Hwang, J. Yoon, T. Yeo, H. H. Son, U. Jeong*, et al.*, "Enhanced critical heat flux with single-walled carbon nanotubes bonded on metal surfaces," *Experimental Thermal and Fluid Science,* vol. 60, pp. 138-147, 2015.

[26] E. J. T. Pialago, O. K. Kwon, J. S. Jin, and C. W. Park, "Nucleate pool boiling of R134a on cold sprayed Cu–CNT–SiC and Cu–CNT–AlN composite coatings," *Applied Thermal Engineering,* vol. 103, pp. 684-694, 2016.

[27] M. Ray, S. Deb, and S. Bhaumik, "Pool boiling heat transfer of refrigerant R-134a on TiO2 nano wire arrays surface," *Applied Thermal Engineering,* vol. 107, pp. 1294-1303, 2016.

[28] H. S. Jo, T. G. Kim, J.-G. Lee, M.-W. Kim, H. G. Park, S. C. James*, et al.*, "Supersonically sprayed nanotextured surfaces with silver nanowires for enhanced pool boiling," *International Journal of Heat and Mass Transfer,* vol. 123, pp. 397-406, 2018.

[29] S. Lee, G. H. Seo, S. Lee, U. Jeong, S. J. Lee, S. J. Kim*, et al.*, "Layer-by-layer carbon nanotube coatings for enhanced pool boiling heat transfer on metal surfaces," *Carbon,* vol. 107, pp. 607-618, 2016.

[30] S. S.-R. S. Jun, A.L. Yarin, "Pool boiling on nano-textured surfaces," *Int. J.Heat Mass Transfer .* vol. 62, pp. 99-111, 2013.

[31] M. W. L. S. Sinha-Ray, S. Sinha-Ray, S. An, B. Pourdeyhimi, S.S. Yoon, A.L. and Yarin, "Supersonic nanoblowing: a new ultra-stiff phase of nylon 6 in 20–50 nm confinement," *J. Mater. Chem,* pp. 3491-3498., 2013.

[32] S. S.-R. R.P. Sahu, S. Sinha-Ray, A.L. Yarin, " Pool boiling on nano-textured surfaces comprised of electrically-assisted supersonically solution-blown,copper-plated nanofibers: experiments and theory,," *Int. J. Heat Mass Transfer* vol. 87, pp. 521–535, 2015.

[33] J. Huang and T. You, "Electrospun nanofibers: from rational design, fabrication to electrochemical sensing applications," in *Advances in nanofibers*, ed: IntechOpen, 2013.

[34] S. J. K. a. F. McClintock, "Describing Uncertainties in Single-sample Experiments," *Mech. Engineering,* vol. 75, pp. 3–8, 1953.

[35] N. A. Barakat, M. H. El-Newehy, A. S. Yasin, Z. K. Ghouri, and S. S. Al-Deyab, "Ni&Mn nanoparticles-decorated carbon nanofibers as effective electrocatalyst for urea oxidation," *Applied Catalysis A: General,* vol. 510, pp. 180-188, 2016.

[36] N. A. Barakat, M. Motlak, A. A. Elzatahry, K. A. Khalil, and E. A. Abdelghani, "NixCo1− x alloy nanoparticle-doped carbon nanofibers as effective non-precious catalyst for ethanol oxidation," *international journal of hydrogen energy,* vol. 39, pp. 305-316, 2014.

[37] N. G. H. Vachon R.I, Tanger G.E, "Evaluation of constants for the Rohsenow pool-boiling correlation," *J. Heat Transfer,* vol. 90, pp. 239-246, 1968.

[38] N. Zuber, "Hydrodynamic Aspects of Boiling Heat Transfer " *Physicsand Mathematics, US Atomic Energy Commission,* 1959.

[39] S. G. Kandlikar, "A theoretical model to predict pool boiling CHF incorporating effects of contact angle and orientation," *J. Heat Transfer* vol. 123 pp. 1071–1079., 2001.

[40] T. Zhang, X. Wu, and T. Luo, "Polymer nanofibers with outstanding thermal conductivity and thermal stability: Fundamental linkage between molecular characteristics and macroscopic thermal properties," *The Journal of Physical Chemistry C,* vol. 118, pp. 21148-21159, 2014.

[41] R. Rioboo, M. Marengo, S. Dall'Olio, M. Voué, and J. De Coninck, "An innovative method to control the incipient flow boiling through grafted surfaces with chemical patterns," *Langmuir,* vol. 25, pp. 6005-6009, 2009.

[42] B. Bourdon, R. Rioboo, M. Marengo, E. Gosselin, and J. De Coninck, "Influence of the wettability on the boiling onset," *Langmuir,* vol. 28, pp. 1618-1624, 2012.

[43] B. Bourdon, P. Di Marco, R. Riobóo, M. Marengo, and J. De Coninck, "Enhancing the onset of pool boiling by wettability modification on nanometrically smooth surfaces," *International Communications in Heat and Mass Transfer,* vol. 45, pp. 11-15, 2013.

Figures

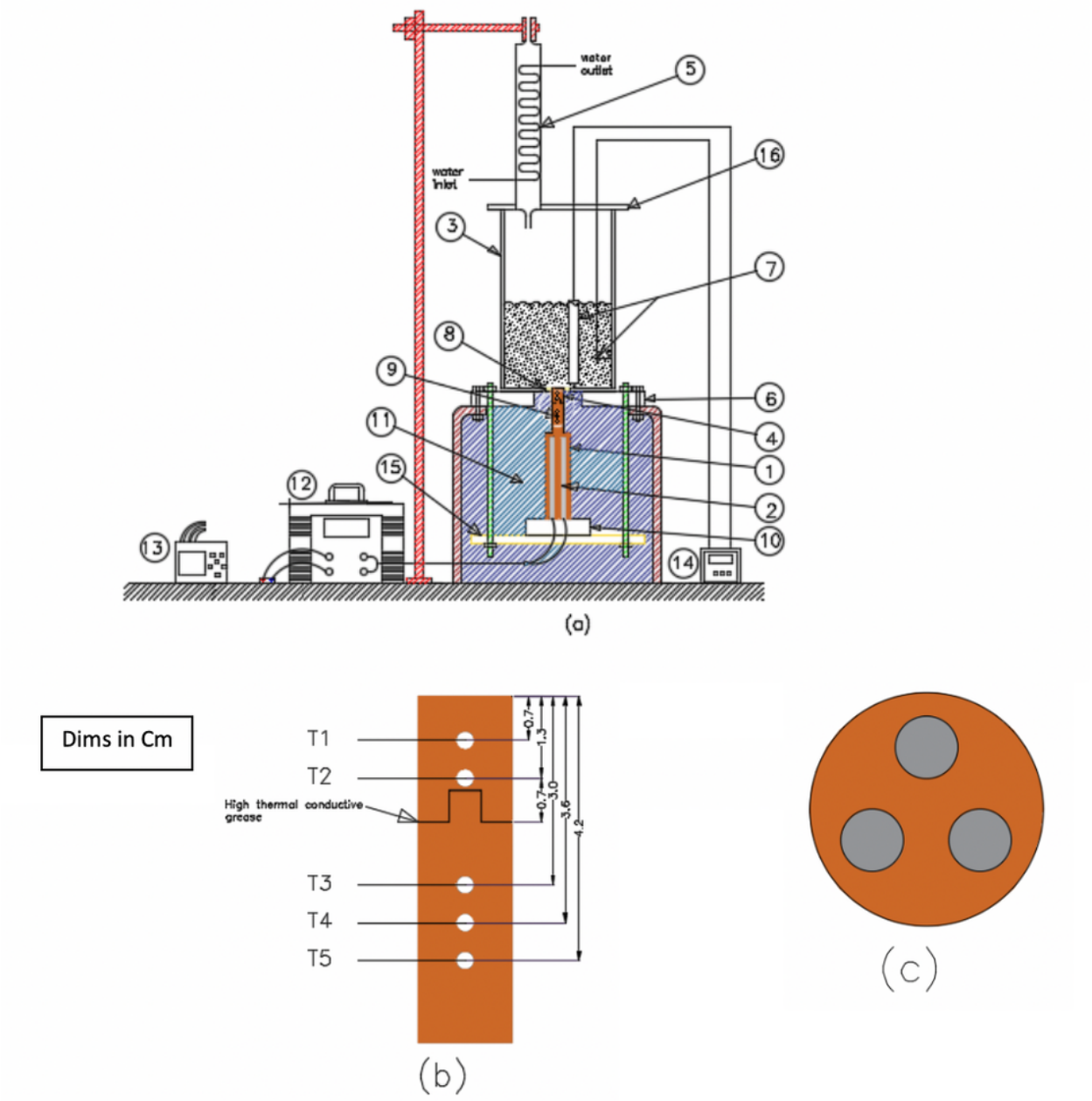

1. Copper rod 2. Cartridge heaters 3. Glass test vessel 4. Copper substrate 5. Glass Condenser 6. Teflon plate insulation 7. Cartridge heater with insulation 8. Teflon ring 9. Thermocouples 10. Ceramic base 11. High temperature thermal insulation 12. Auto transformer 13. Data logger 14. Temperature controller 15. Stainless steel plate 16. Plexiglass plate

Figure 1

A schematic of the experimental setup, (a) along with Locations of thermocouples, (b) and heaters distribution in the copper rod, (c).

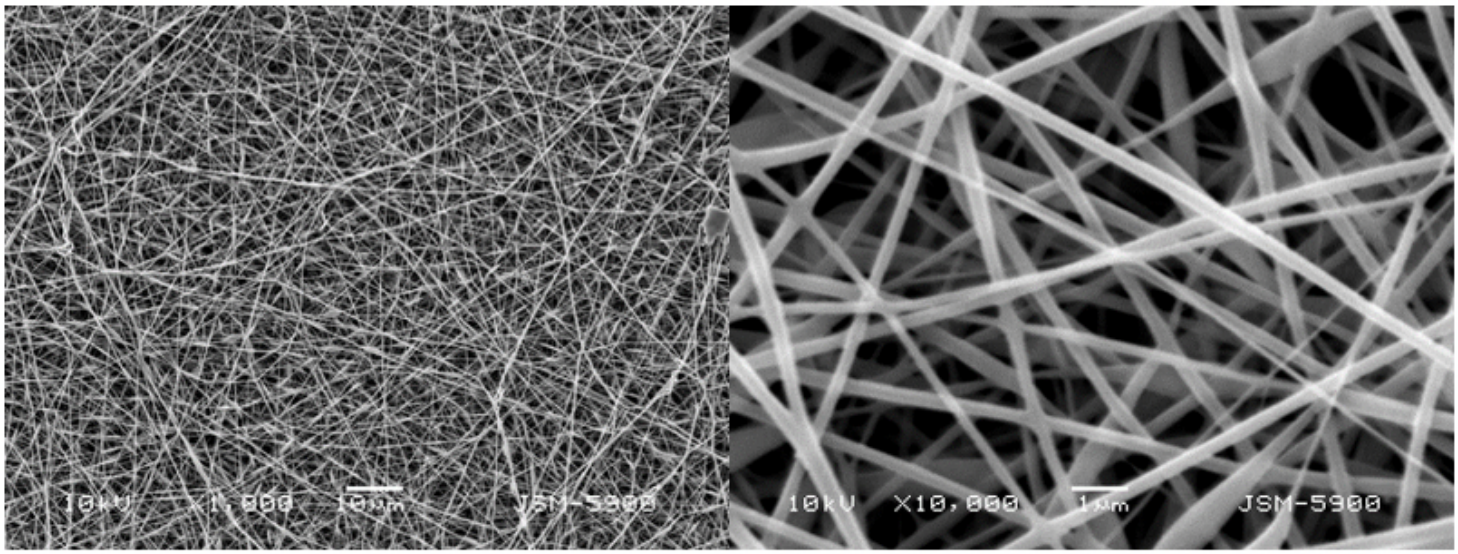

Figure 2

SEM image for the CuAC/PVA electrospun nanofibers.

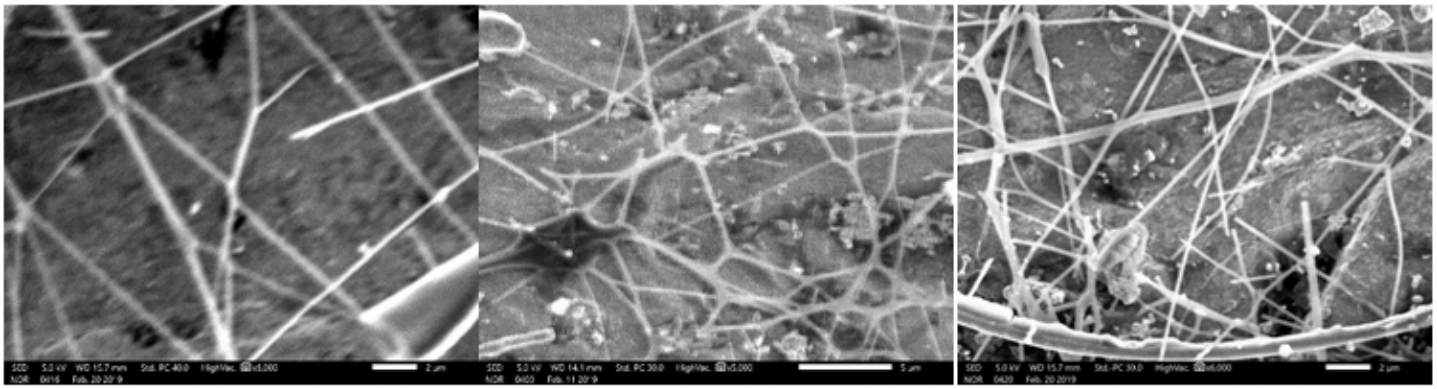

Figure 3

SEM image for the copper disc surfaces coated by CuAc/PVA nanofibers for 5 min (A), 15 min (B) and 30 min (C) after the calcination process.

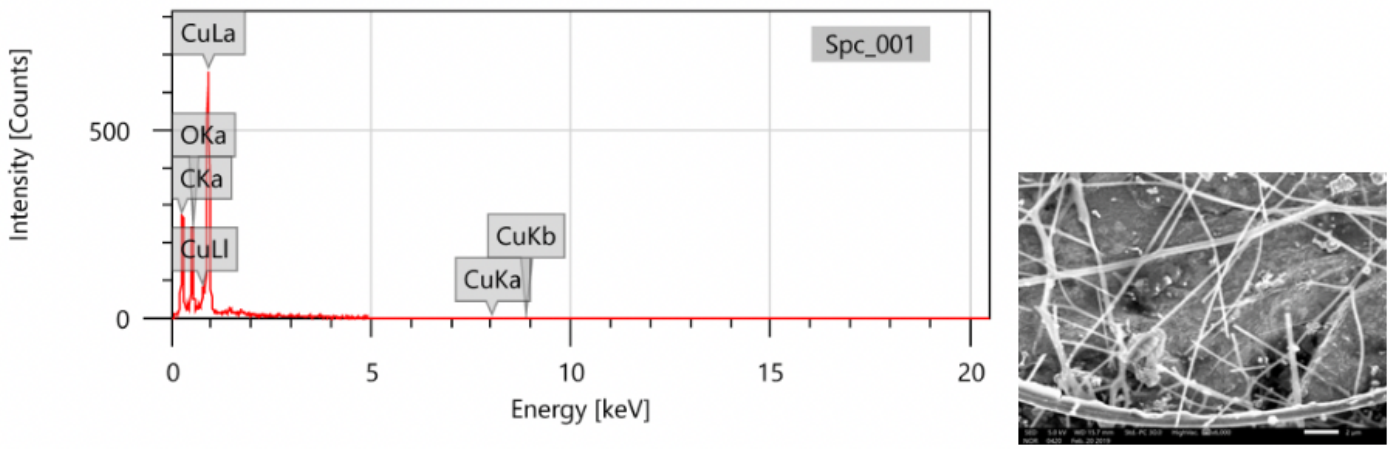

Figure 4

EDX analysis for a randomly selected area from the sample S3 surface

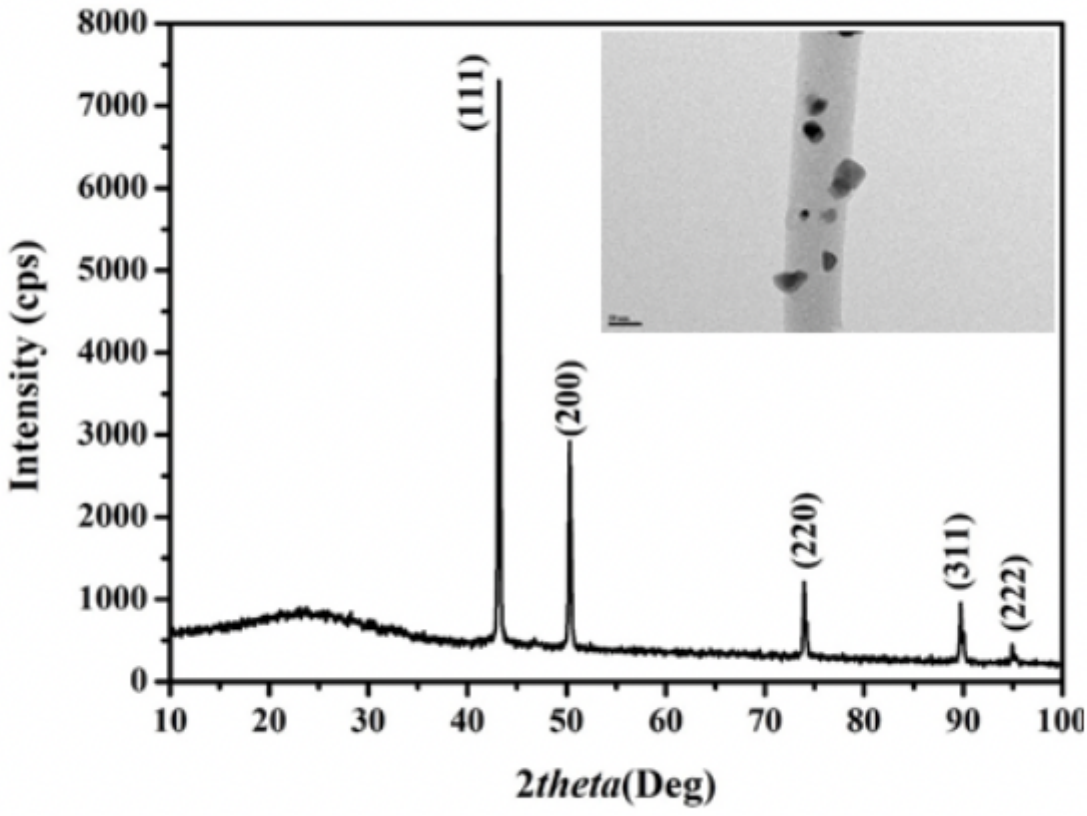

Figure 5

XRD analysis results the powder obtained from calcination of CuAC/PVA electrospun nanofibers (sample S3) at 850 °C. The inset displays TEM image.

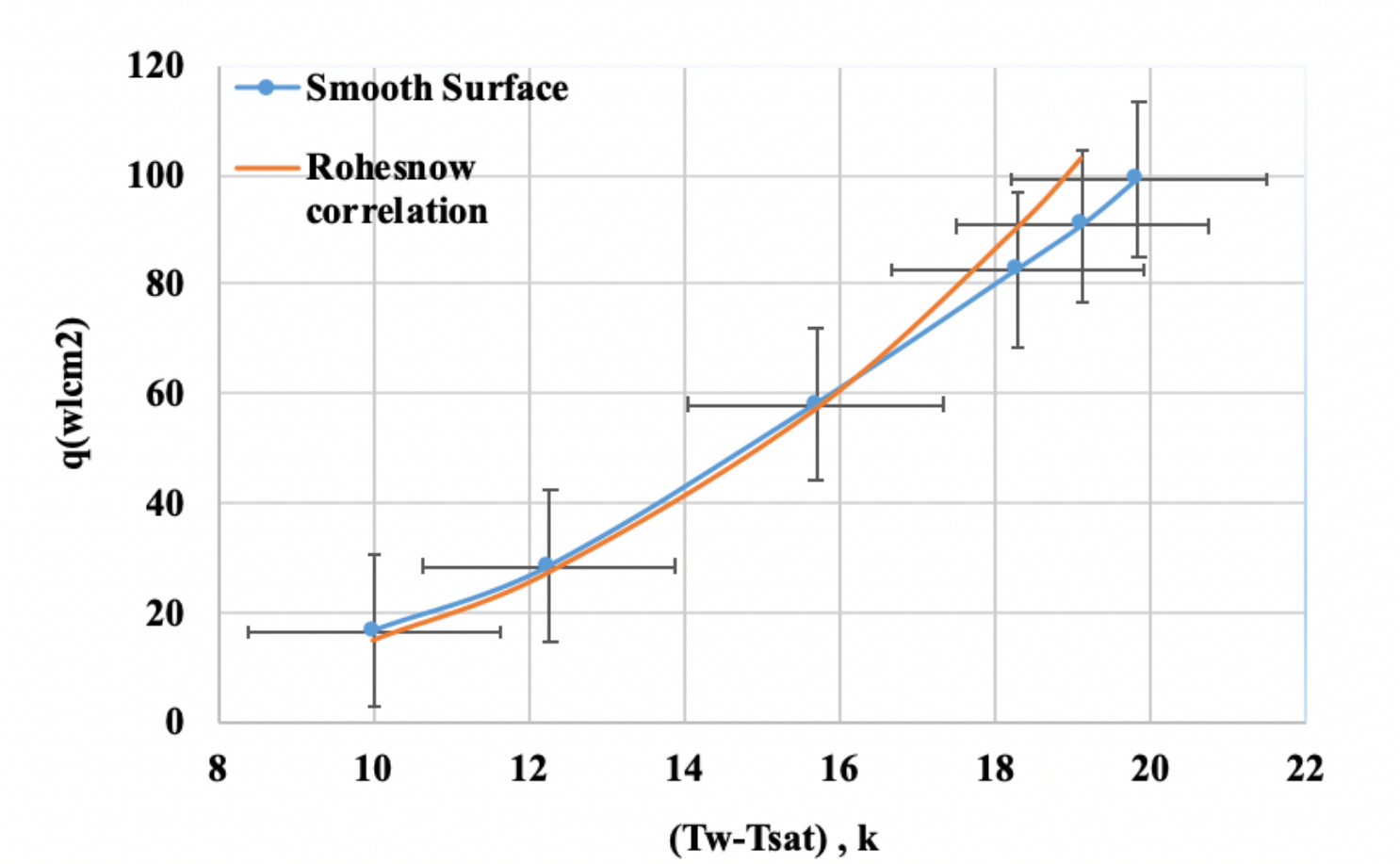

Figure 6

comparing the present results to Rohsenow correlation for smooth copper surface.

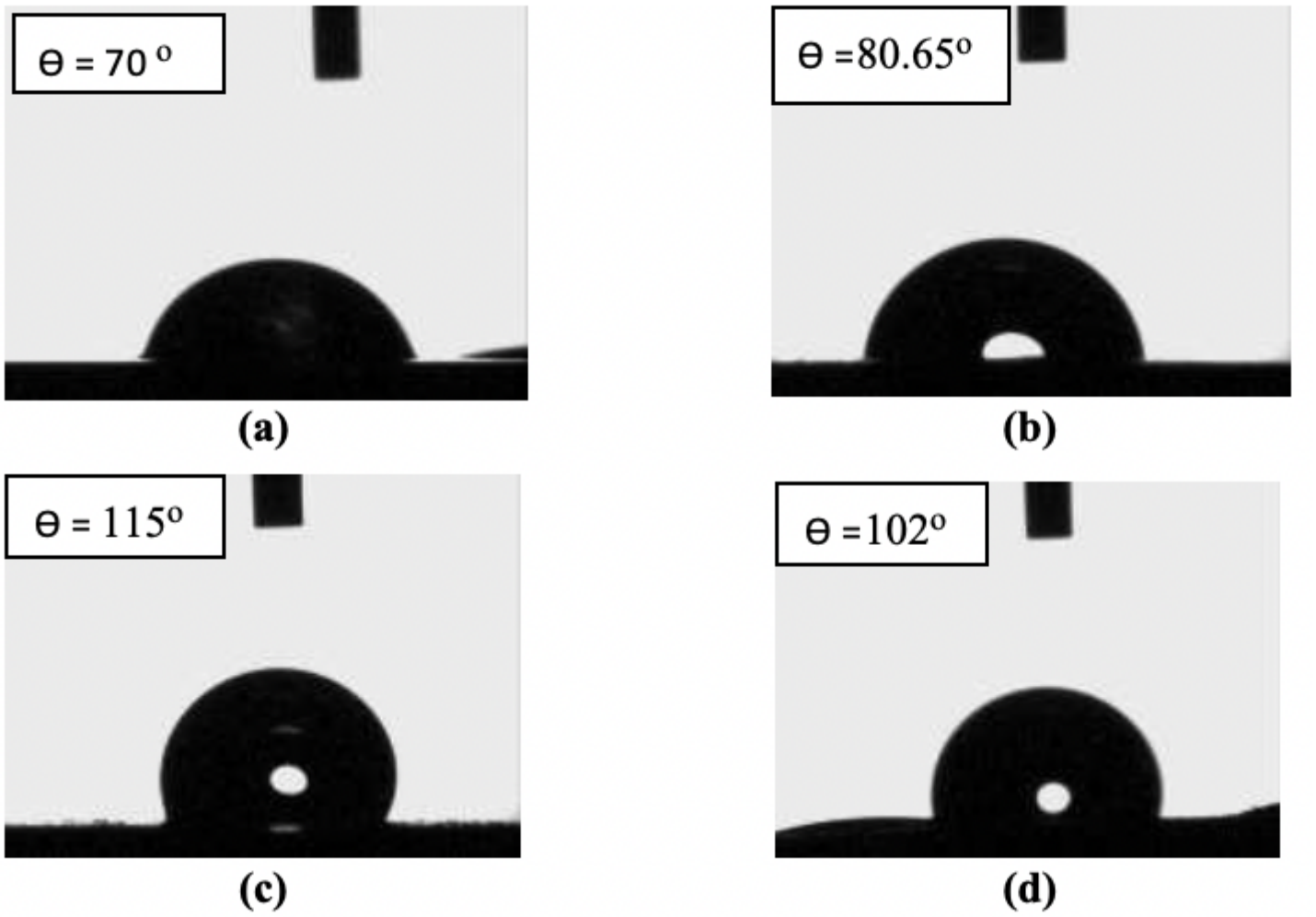

Figure 7

Contact angles of the nanostructured surfaces: (a) for smooth surface, (b), (c) and (d) for S1, S2 and S3 respectively.

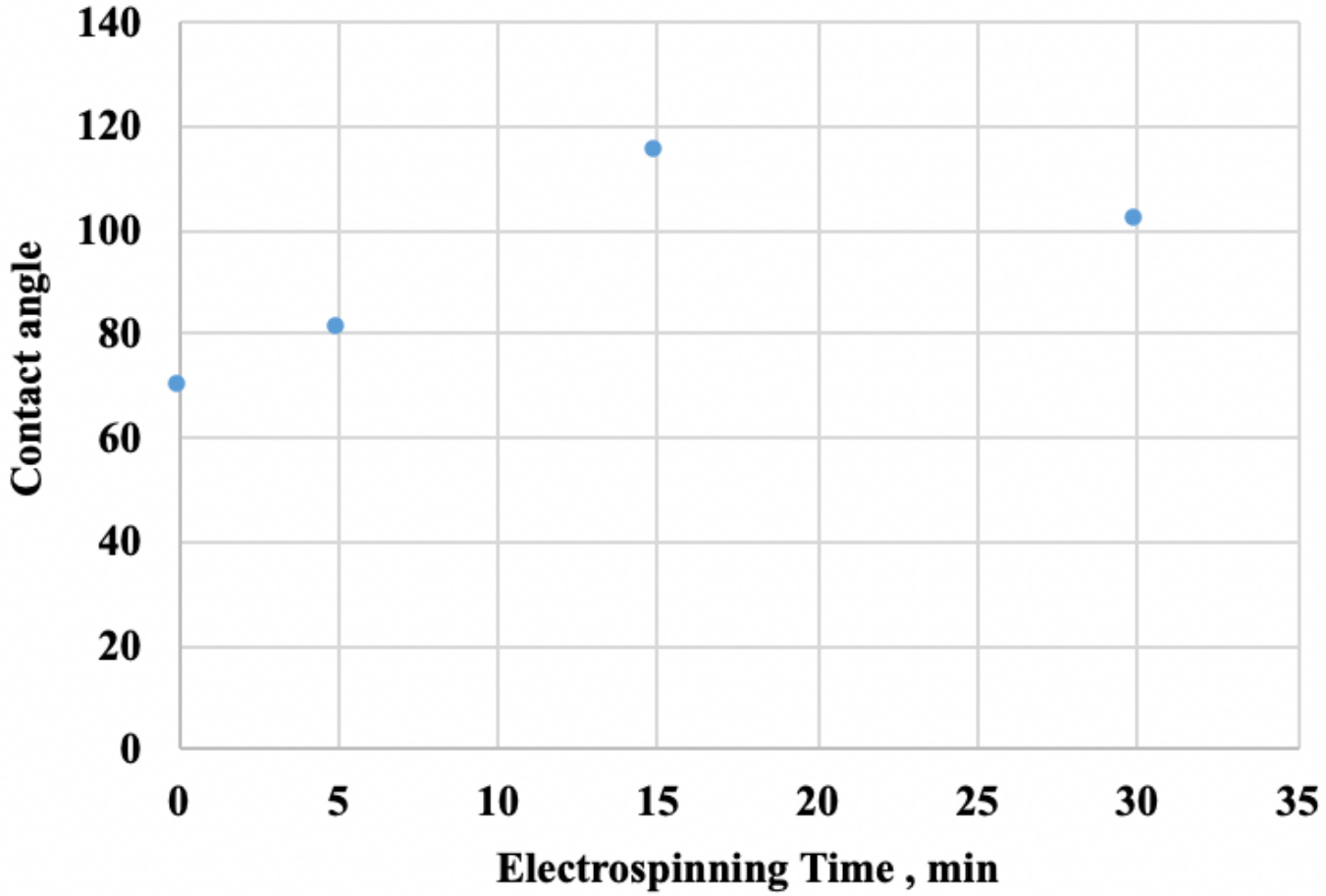

Figure 8

Effect of electro spinning time on contact angles

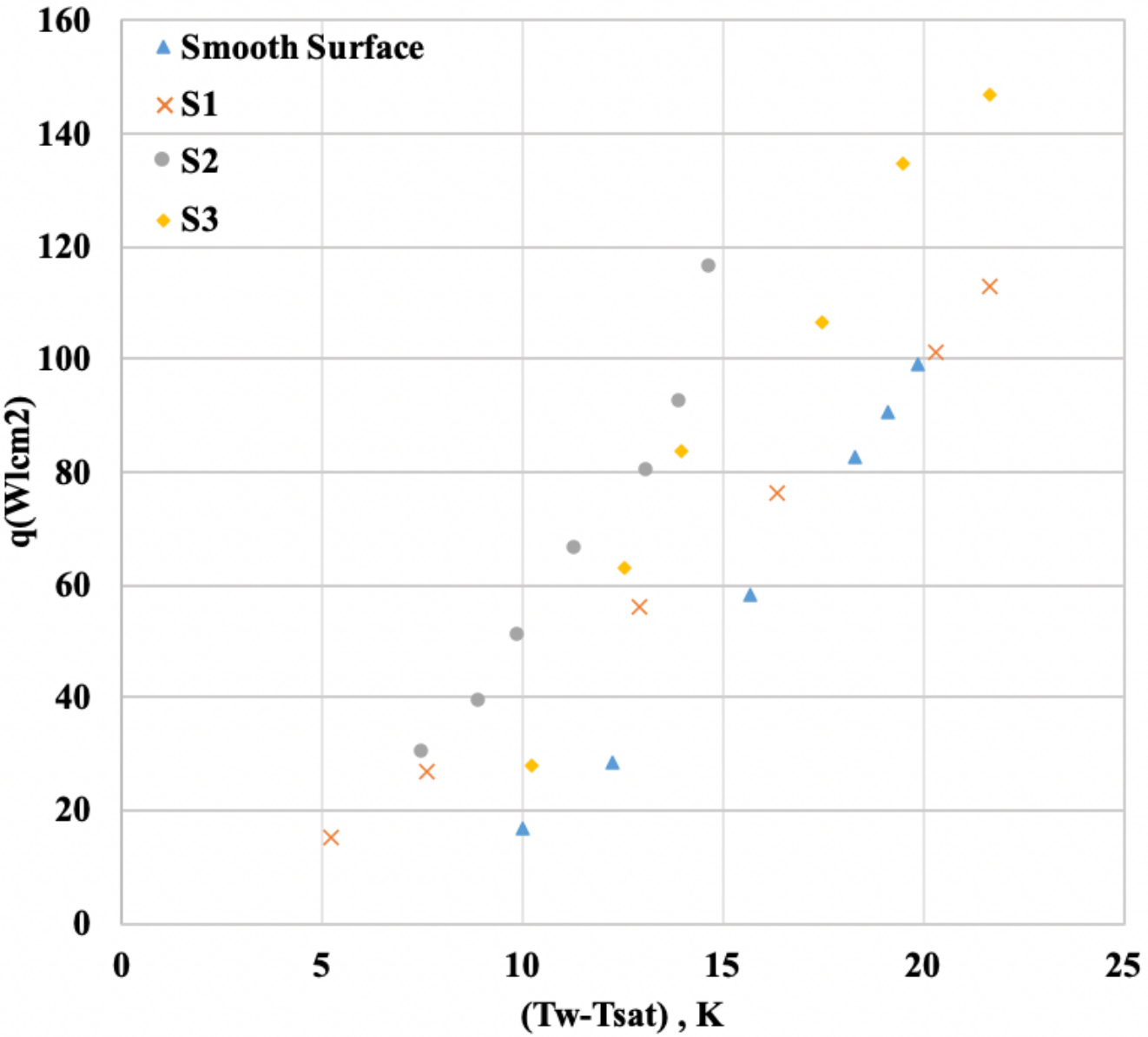

Figure 9

Boiling curves of heat flux versus wall superheat for a smooth surface baseline compared to nanostructured surfaces.

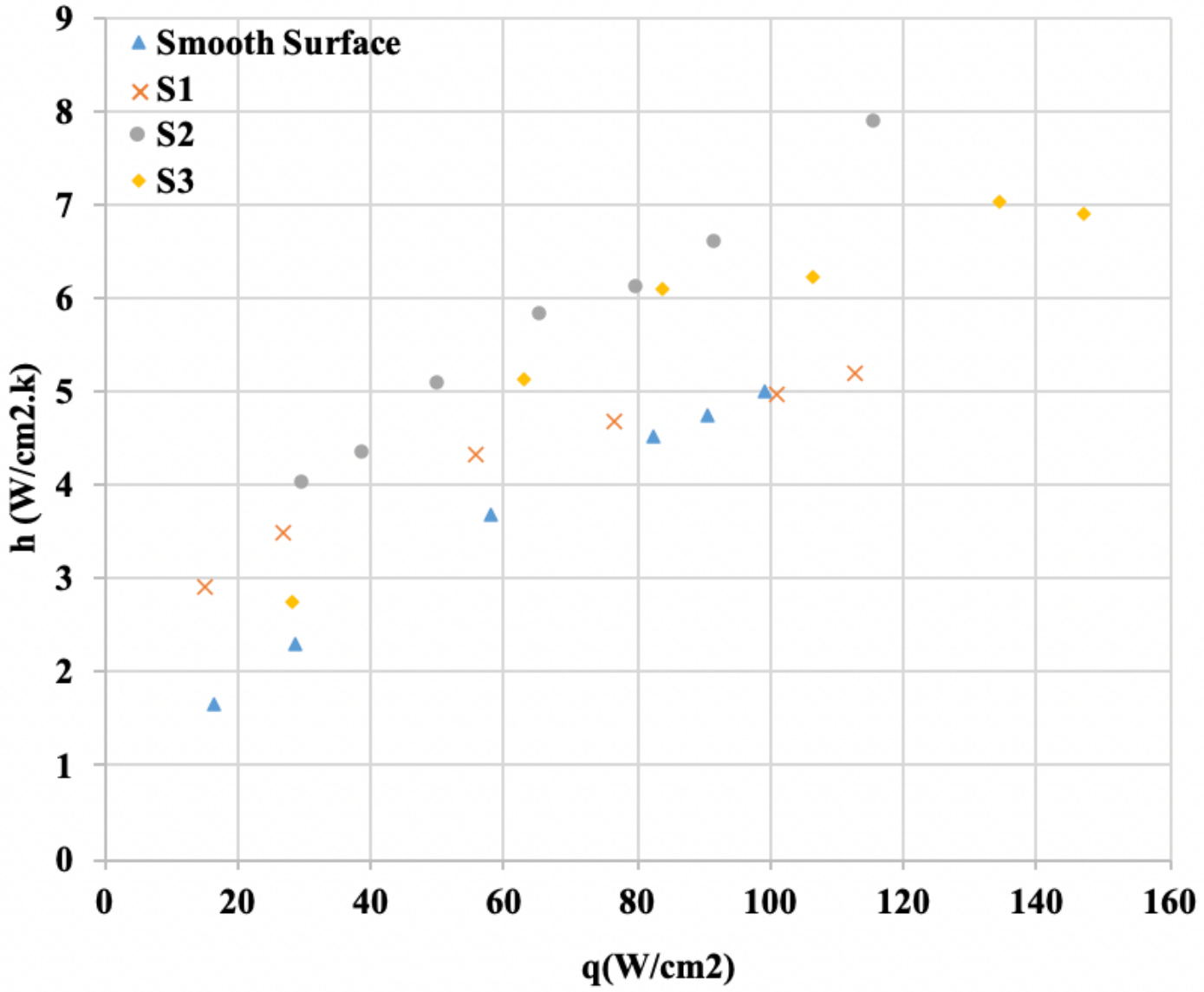

Figure 10

Variation of heat transfer coefficient (h) against heat flux (q) for nanostructured surfaces compared to smooth surface

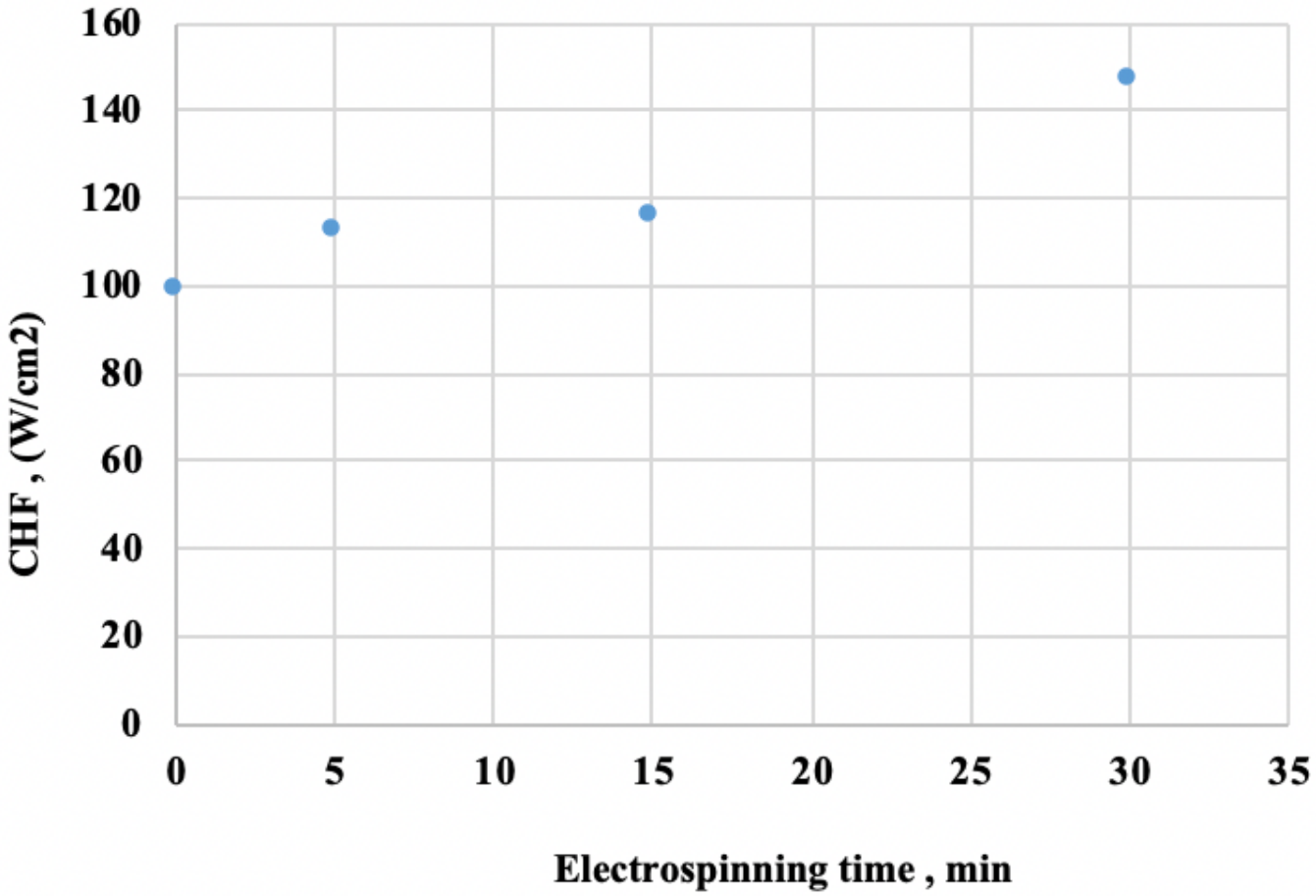

Figure 11

Relation between CHF and electrospinning time